

Density of amorphous Si

J. S. Custer and Michael O. Thompson

Department of Materials Science and Engineering, Cornell University, Ithaca, New York 14853

D. C. Jacobson and J. M. Poate

AT&T Bell Laboratories, Murray Hill, New Jersey 07974

S. Roorda and W. C. Sinke

FOM—Institute for Atomic and Molecular Physics, 1098 SJ Amsterdam, The Netherlands

F. Spaepen

Division of Applied Sciences, Harvard University, Cambridge, Massachusetts 02138

(Received 10 September 1993; accepted for publication 21 October 1993)

The density of amorphous Si has been measured. Multiple Si implants, at energies up to 8.0 MeV, were made through a contact mask to produce alternating amorphous/crystalline Si stripes with amorphous thicknesses up to $\sim 5.0 \mu\text{m}$. For layers up to $3.4 \mu\text{m}$ (5 MeV), the amorphous Si is constrained laterally and deforms plastically. Above 5 MeV, plastic deformation of the surrounding crystal matrix is observed. Height differences between the amorphous and crystalline regions were measured for as-implanted, thermally relaxed, and partially recrystallized samples using a surface profilometer. Combined with ion channeling measurements of the layer thickness, amorphous Si was determined to be $1.8 \pm 0.1\%$ less dense than crystalline Si ($4.90 \times 10^{22} \text{ atom/cm}^3$ at 300 K). Both relaxed and unrelaxed amorphous Si show identical densities within experimental error ($< 0.1\%$ density difference).

Many basic properties of amorphous Si (*a*-Si) are not known despite continuing technological and scientific interest. One such fundamental property, critical for testing microscopic models, is the density of amorphous Si relative to the crystalline phase. Early x-ray diffraction data indicated an amorphous density as much as 10% below that of the crystal, although this was attributed to the presence of voids in the vapor-deposited films.¹ Brodsky, Kaplan, and Ziegler interpreted Rutherford backscattering measurements in combination with surface profilometry to conclude that *a*-Si could be up to 1% denser than crystalline Si (*c*-Si), although the measured density of their electron-beam deposited *a*-Si films was 3% less dense than *c*-Si.² Direct density measurements using weighing and interferometry of *a*-Ge deposited at the highest possible temperature indicated a density 1% greater than *c*-Ge.³ Most recently, experimental results on thin implanted layers indicate an *a*-Si density between 1.7% and 2.3% less than the crystal.⁴ Theoretical and computer models of the structure of *a*-Si, assuming a continuous random network (CRN) without point defects, predict that the amorphous phase should be 3%–4% more dense than the crystal.⁵ Subsequent attempts to estimate the density of *a*-Si using molecular-dynamics simulations have led to results on either side of *c*-Si.⁶ As seen from these previous results, not only is the density difference unknown, there continues to be debate over the sign of the difference.

Although it is generally accepted that the best characterized amorphous state is formed by ion implantation, it is known that this state is not unique. The unrelaxed *a*-Si produced by ion implantation releases substantial enthalpy during low-temperature annealing toward a relaxed configuration.^{7–9} It is unclear, however, if this relaxation affects other physical properties, such as the density.

In this letter we report measurements of the density of

self-implanted amorphous Si layers over a wide range of thickness, regrowth, and relaxation conditions. Alternating stripes of *a*-Si ($\sim 300 \mu\text{m}$ wide) and *c*-Si ($\sim 100 \mu\text{m}$) were produced by MeV Si ion implantation through a steel mask into (100) Si on a National Electrostatics Corporation 1.7-MeV tandem accelerator. Such implantations are known to produce thick, well-characterized (thermodynamically and kinetically) *a*-Si.^{7,10} The relative density was then determined by measuring the physical step height at lateral *a*-Si/*c*-Si boundaries. Implants were performed at energies from 0.5 to 8.0 MeV; energies, doses, and *a*-Si thicknesses for each implant series are shown in Table I. Each higher-energy implant included all lower-energy implants to ensure surface amorphization. All irradiations, except one, were performed with samples heat-sunk with vacuum grease to a copper block nominally held at 77 K. One sample was implanted instead at room temperature to check for density variations caused by the implant conditions. Various *a*-Si thicknesses were obtained by partially recrystallizing implanted layers at 580 °C in a vacuum annealing furnace with a base pressure of $\sim 10^{-7}$ Torr. To test for possible changes in the density

TABLE I. Description of amorphizing Si implants, including energy of each implant, dose at that energy, thickness of material implanted to that point, and thickness of the amorphous layer made to that energy.

Energy (MeV)	Dose ($10^{15}/\text{cm}^2$)	Net material added (nm)	<i>a</i> -Si thickness as implanted (μm)
0.5	5.0	0.6	0.9
1.0	5.0	1.4	1.4
2.0	5.0	2.3	2.1
3.5	6.0	3.3	2.9
5.0	7.0	4.7	3.4
6.5	8.0	6.2	4.3
8.0	8.0	7.7	5.0

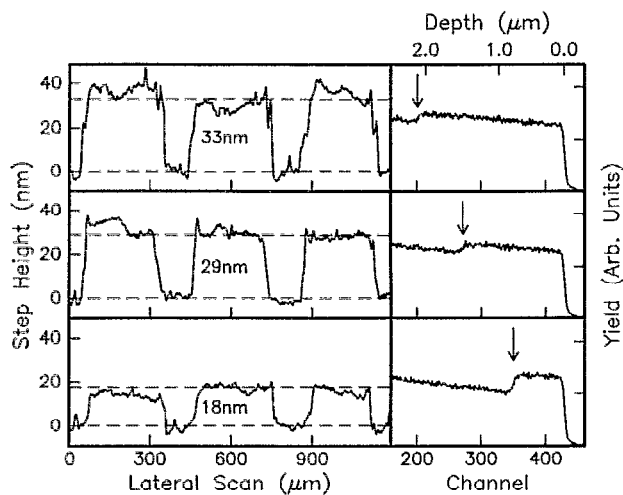


FIG. 1. (a) Surface profilometer traces of 2.1-, 1.5-, and 0.8- μm -thick *a*-Si layers produced by 0.5–2.0-MeV series implants and epitaxial recrystallization. (b) Channeling spectra of samples shown in (a). The *a*-Si thicknesses are indicated.

with relaxation, a section of each as-implanted sample was thermally relaxed by annealing for 1 h at 500 °C.

Areal densities (atom/cm²) of the *a*-Si layers were measured by Rutherford backscattering spectrometry (RBS) in the channeling configuration using 3-MeV ⁴He. Measurements of the total energy loss in the *a*-Si layer were converted to areal densities using the ⁴He stopping powers in Si (ϵ). Thicknesses were then obtained by dividing by the approximate density ($\sim 4.9 \times 10^{22}$ atom/cm³). For *a*-Si films $> 2.8 \mu\text{m}$, thicknesses were estimated by RBS channeling measurements after partial solid-phase epitaxy (SPE); dechanneling in the *a*-Si prevented direct measurement beyond $\sim 2.8 \mu\text{m}$. The resulting annealed thicknesses were extrapolated back to the original thickness using known epitaxial crystallization kinetics.¹⁰ Unfortunately, there are two accepted sets of experimental measurements for ϵ which differ by up to 6% from each other.^{11,12} Since this represents a systematic error substantially larger than any other error in the measurement, results are presented using both sets.

Surface profiles of the alternating *a*-Si and *c*-Si lines were obtained for each sample using a Tencor Instruments Alpha-step 200 surface profilometer calibrated with an NIST traceable standard. Digitized height measurements on 1- μm spacings over a 2000- μm lateral distance (\approx four periods) were obtained. Figure 1(a) shows example scans for an 2.1- μm (as-implanted) layer and for other thicknesses obtained by SPE from this implant; corresponding RBS channeling spectra are shown in Fig. 1(b). The high regions in the profilometer traces were identified as *a*-Si by both visual observation of the higher reflectivity of *a*-Si (Ref. 13) and by the relative linewidths of the implant mask. This unambiguously shows that *a*-Si is less dense than *c*-Si.

Each *c*-Si/*a*-Si/*c*-Si step was analyzed by first fitting a parabola through the *c*-Si regions to compensate for wafer tilt and simple curvature, and then determining the average step height. Typically, three scans were made on each sample, and the reported values are an average of twelve

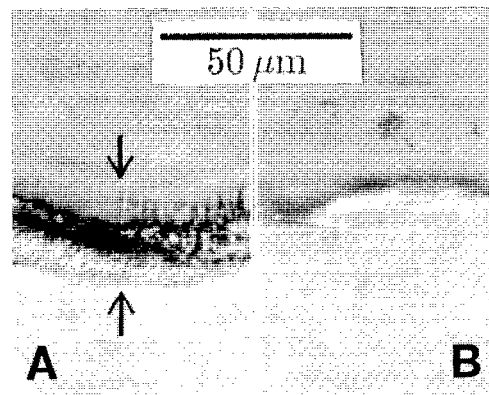


FIG. 2. Optical micrographs of the lateral *a*-Si/*c*-Si edge after a Wright Jenkins etch of (A) a sample implanted at energies 0.5–8.0 MeV showing a large deformation zone (between arrows) and (B) a sample implanted from 0.5 to 5.0 MeV showing little deformation. The top region is *c*-Si and the lower region is etched *a*-Si.

individual steps. The variance of each data set was typically 3.5 nm, independent of the absolute step height. The errors, however, were nonrandom; if step heights within each scan were averaged, the collection of averages showed variances much smaller than expected. This suggests that the variance is dominated by instrumental limitations rather than variations in the actual step heights. To estimate the true *a*-Si step-height variance, the instrumental component of the total variance was determined directly by measuring step heights of photolithographically patterned 20- and 40-nm SiO₂ layers on *c*-Si. These measurements, with a true sample variance near zero, also showed a variance of 3.5 nm. Consequently, the observed variance is predominantly instrumental, and, while the variation of actual *a*-Si step heights cannot be determined, it must be less than 2 nm.

A small correction was made to the measured step heights to account for the Si implanted and sputtered¹⁴ during amorphization. These corrections, listed in Table I, were determined by dividing the net implant dose (implant minus sputtering) by the atomic density of *c*-Si. For example, the 2.0-MeV implant itself adds 1.0 nm while sputtering removes 0.15 nm, giving a net addition of 0.85 nm.

Interpreting step heights as a density difference requires understanding how the volume change is accommodated. Amorphous Si can form with built-in stresses, the substrate can plastically deform, or the *a*-Si can plastically deform during implantation. Measurements on laterally continuous 1- μm *a*-Si layers demonstrate that the volume change is primarily accommodated by a vertical strain with the in-plane strain less than 1% of the total strain.¹⁵ This indicates that *a*-Si deforms plastically during formation by ion implantation. In the constrained geometry of these experiments, plastic deformation of *a*-Si occurs for implants below 5 MeV and the entire volume change is exhibited as a vertical expansion. However, for the higher-energy implants, plastic deformation of the constraining *c*-Si can be readily observed as shown in Fig. 2. As-implanted 0.5–5 and 0.5–8 MeV samples were treated for 15 s in a Wright Jenkins etch to highlight defects and remove *a*-Si.¹⁶ A dense plastic deformation zone is revealed at the *c*-Si edge for the 0.5–8-MeV

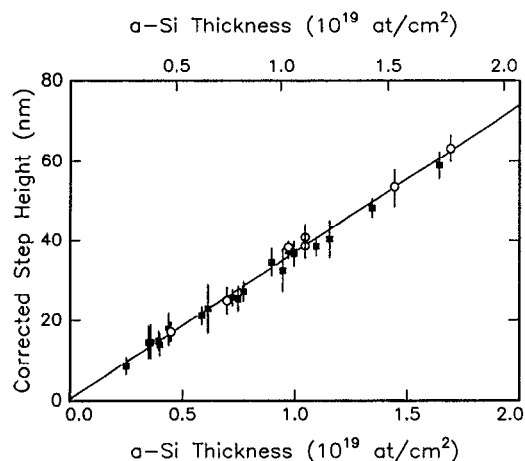


FIG. 3. Corrected step height vs *a*-Si areal density for as-implanted samples (open circles) and annealed samples (filled squares) of all implant series from 0.5 to 5.0 MeV. The areal density was obtained using the stopping powers of either Ziegler (Ref. 11, bottom axis) or Santry and Werner (Ref. 12, top axis). The solid line shows the step height expected for a 1.73% density difference (Santry and Werner values).

implant series. Although some minor deformation occurs for 5-MeV (or lower energy) samples, it is on a sharply reduced scale. As a result of *c*-Si deformation, volume expansion of *a*-Si occurs both laterally and vertically for high-energy implants and measured step heights for 0.5–6.5- and 0.5–8-MeV implants were thus not used in determining the density.

The step-height data are shown in Fig. 3 versus the areal densities of the *a*-Si layers. As-implanted samples are shown by the open circles and partially recrystallized or relaxed samples by filled squares; errors shown are predominantly instrumental in origin. Within these errors, step heights measured for the room-temperature-implanted sample were identical to those measured on samples implanted at liquid-nitrogen temperature. In addition, no differences in density could be detected between unrelaxed, relaxed, or regrown samples, nor between samples implanted at any energy up to 5 MeV. Converting the areal density (using Santry and Werner stopping powers¹²) to the *a*-Si thickness and fitting a least-squares line (with consideration for the individual error bars) through all the data yield a density difference of $1.74 \pm 0.06\%$. Fitting only as-implanted (unrelaxed) samples, the density difference is $1.79 \pm 0.13\%$, while for annealed (i.e., relaxed) samples it is $1.70 \pm 0.07\%$. Thus there is no statistically significant difference between the density of as-implanted and annealed (relaxed) *a*-Si. The linear fit to the entire set shows an intercept of 0.8 ± 1.1 nm, confirming that the correction for implanted material is valid. Table II compares the least-squares fits determined using both sets of ⁴He stopping powers. Considering the relative and absolute uncertainties in the stopping-power measurements, an average value of $1.8 \pm 0.1\%$ is our best estimate for the difference between the *a*-Si and *c*-Si densities.

In conclusion, we have determined that *a*-Si is $1.8 \pm 0.1\%$ less dense than *c*-Si. There are several consequences

TABLE II. Parameters for linear fits to all the samples, the as-annealed samples, and the as-implanted samples using the stopping powers of either Ziegler (Ref. 11) or Santry and Werner (Ref. 12) to obtain the *a*-Si thickness.

	Ziegler stopping powers		Santry and Werner	
	Slope (%)	Offset (nm)	Slope (%)	Offset (nm)
All	1.83 ± 0.06	1.0 ± 1.1	1.74 ± 0.06	0.8 ± 1.1
As-implanted	1.86 ± 0.13	1.5 ± 2.8	1.79 ± 0.13	0.8 ± 2.8
As-annealed	1.79 ± 0.07	1.2 ± 1.2	1.70 ± 0.07	1.1 ± 1.2

of this result. First, simple fully coordinated CRN models cannot be correct since they yield the wrong sign for the density difference. Second, since there is no measurable density difference between as-implanted and annealed samples, the relaxation observed in calorimetry,^{7,8} optical,¹⁷ and Raman¹⁸ measurements occurs without significant volume changes. A detailed microscopic model of amorphous Si thus remains to be developed.

We are indebted to C. A. Volkert, S. Hyland, and D. J. Eaglesham for assistance and helpful discussions. The work at Cornell was supported by NSF-PYIA (J. Hurt) and the SRC through the Cornell Microscience & Technology Program (Contract No. 89-SC-069). The work at Harvard is supported by the NSF through the Materials Research Laboratory. We also acknowledge R. Boyko and R. Soave and the Cornell National Nanofabrication Facility (NSF).

- ¹S. C. Moss and J. F. Graczyk, Phys. Rev. Lett. **23**, 1167 (1969).
- ²M. H. Brodsky, D. Kaplan, and J. F. Ziegler, Appl. Phys. Lett. **21**, 305 (1972).
- ³T. M. Donovan, E. J. Ashley, and W. E. Spicer, Phys. Lett. **32A**, 85 (1970).
- ⁴W. G. Spitzer, G. K. Hubler, and T. A. Kennedy, Nucl. Instrum. Methods **209/210**, 309 (1983).
- ⁵F. Wooten and D. Weaire, Solid State Phys. **40**, 1 (1987).
- ⁶W. D. Luedtke and U. Landman, Phys. Rev. B **40**, 1164 (1989).
- ⁷E. P. Donovan, F. Spaepen, J. M. Poate, and D. C. Jacobson, Appl. Phys. Lett. **55**, 1516 (1989).
- ⁸S. Roorda, S. Doorn, W. C. Sinke, P. M. L. O. Scholte, and E. van Loenen, Phys. Rev. Lett. **62**, 1880 (1989).
- ⁹S. Roorda, W. C. Sinke, J. M. Poate, D. C. Jacobson, S. Dierker, B. S. Dennis, D. J. Eaglesham, F. Spaepen, and P. Fuoss, Phys. Rev. B **44**, 3702 (1991).
- ¹⁰J. A. Roth, G. L. Olson, D. C. Jacobson, and J. M. Poate, Appl. Phys. Lett. **57**, 1340 (1990).
- ¹¹J. F. Ziegler, *He Stopping Powers and Ranges in all Elemental Matter* (Pergamon, New York, 1978).
- ¹²D. C. Santry and R. D. Werner, Nucl. Instrum. Methods **159**, 523 (1979); D. C. Santry and R. D. Werner, *ibid.* **178**, 523 (1980).
- ¹³G. L. Olson and J. A. Roth, Mater. Sci. Rep. **3**, 1 (1988).
- ¹⁴P. Sigmund, Phys. Rev. **184**, 383 (1969).
- ¹⁵C. A. Volkert, J. Appl. Phys. **70**, 3521 (1991).
- ¹⁶Margaret Wright Jenkins, J. Electrochem. Soc. **124**, 757 (1977).
- ¹⁷J. E. Fredrickson, C. N. Waddell, W. G. Spitzer, and G. K. Hubler, Appl. Phys. Lett. **40**, 172 (1982).
- ¹⁸R. Tsu, J. G. Hernandez, and F. H. Pollak, J. Non-Cryst. Solids **66**, 109 (1984); W. C. Sinke, T. Warabisako, M. Miyao, T. Tokuyama, S. Roorda, and F. W. Saris, J. Non-Cryst. Solids **99**, 308 (1988).